

## 磁性 Y-MOF@SiO<sub>2</sub>@Fe<sub>3</sub>O<sub>4</sub> 催化剂的制备及其 在 Aza-Michael 加成反应中的性能

穆金城<sup>1,2</sup> 蒋 赛<sup>1</sup> 季生福<sup>\*,1</sup>

(<sup>1</sup> 北京化工大学化工资源有效利用国家重点实验室, 北京 100029)

(<sup>2</sup> 塔里木大学兵团南疆化工资源利用工程实验室, 阿拉尔 843300)

**摘要:** 在磁性 SiO<sub>2</sub>@Fe<sub>3</sub>O<sub>4</sub> 纳米微球表面原位合成包覆不同含量的 Y-MOF, 从而制备出新型磁性 Y-MOF@SiO<sub>2</sub>@Fe<sub>3</sub>O<sub>4</sub> 催化剂。采用 XRD、TEM、FT-IR、VSM 和 N<sub>2</sub> 吸附-脱附测试等手段对催化剂的结构进行表征, 并且评价了催化剂对苯胺和丙烯酸甲酯的 Aza-Michael 加成反应性能。结果表明 Y-MOF 能均匀包覆在磁性 SiO<sub>2</sub>@Fe<sub>3</sub>O<sub>4</sub> 纳米微球表面, 形成具有核壳结构的磁性 Y-MOF@SiO<sub>2</sub>@Fe<sub>3</sub>O<sub>4</sub> 催化剂, 催化剂具有良好的超顺磁性。Y-MOF 含量为 43.3%(w/w) 的 Y-MOF@SiO<sub>2</sub>@Fe<sub>3</sub>O<sub>4</sub> 催化剂, 在苯胺和丙烯酸甲酯的 Aza-Michael 加成反应表现出最好的催化性能, 丙烯酸甲酯的转化率为 88.3% 时, *N*-(β-甲氧羰乙基)苯胺的选择性可达 99.8%。反应后的催化剂可以通过外磁场容易回收, 并且重复使用 5 次其转化率和选择性没有明显下降。

**关键词:** 磁性; Y-MOF@SiO<sub>2</sub>@Fe<sub>3</sub>O<sub>4</sub>; 催化剂; Aza-Michael 反应

中图分类号: O643.36 文献标识码: A 文章编号: 1001-4861(2018)09-1753-08

DOI: 10.11862/CJIC.2018.209

## Preparation and Properties for Aza-Michael Addition Reaction of Magnetic Y-MOF@SiO<sub>2</sub>@Fe<sub>3</sub>O<sub>4</sub> Catalysts

MU Jin-Cheng<sup>1,2</sup> JIANG Sai<sup>1</sup> JI Sheng-Fu<sup>\*,1</sup>

(<sup>1</sup>State Key Laboratory of Chemical Resource Engineering, Beijing University of Chemical Technology, Beijing 100029, China)

(<sup>2</sup>Engineering Laboratory of Chemical Resources Utilization in South Xinjiang of XPCC,  
Tarim University, Alar, Xinjiang 843300, China)

**Abstract:** The magnetic Y-MOF@SiO<sub>2</sub>@Fe<sub>3</sub>O<sub>4</sub> catalysts with different Y-MOF contents were synthesized by encapsulating magnetic SiO<sub>2</sub>@Fe<sub>3</sub>O<sub>4</sub> nanospheres into Y-MOF through an *in-situ* method. The structure of the catalyst was characterized by X-ray diffraction (XRD), transmission electron microscopy (TEM), infrared spectroscopy (FT-IR), vibration sample magnetometer (VSM) and the N<sub>2</sub> adsorption-desorption test. The performance of the catalyst for Aza-Michael addition reaction with aniline and methyl acrylate was evaluated. The results showed that Y-MOF was uniformly coated on the surface of the SiO<sub>2</sub>@Fe<sub>3</sub>O<sub>4</sub> nanospheres to form a core-shell magnetic Y-MOF@SiO<sub>2</sub>@Fe<sub>3</sub>O<sub>4</sub> catalyst. The catalysts exhibited good superparamagnetism. When Y-MOF content was 43.3% (w/w), the Y-MOF@SiO<sub>2</sub>@Fe<sub>3</sub>O<sub>4</sub> catalyst had better catalytic performance for the Aza-Michael addition reaction. The conversion of methyl acrylate was 88.3% and the selectivity of *N*-(β-methoxycarbonyl)ethyl aniline was 99.8%. After reaction, the catalyst was recovered by magnetic recovery. It was reused five times, and still has high conversion and selectivity.

**Keywords:** magnetic; Y-MOF@SiO<sub>2</sub>@Fe<sub>3</sub>O<sub>4</sub>; catalyst; Aza-Michael reaction

收稿日期: 2018-05-11。收修改稿日期: 2018-06-27。

国家自然科学基金(No.21573015, 21173018)资助项目。

\*通信联系人。E-mail: jjsf@mail.buct.edu.cn

The Aza-Michael reaction is commonly used in organic synthesis to grow carbon chains. Among them the Aza-Michael addition reaction of the nitrogen nucleophiles and the lack of electron-polymer compounds is an important method for formation of C-N bond<sup>[1-2]</sup>. The addition of  $\alpha$ ,  $\beta$ -unsaturated carbonyl compounds is an effective way to synthesize  $\beta$ -amino-carbonyl compounds<sup>[3]</sup>. The  $\beta$ -aminocarbonyl compounds can be further converted to  $\beta$ -amino acids and  $\beta$ -lactam. These compounds can be further synthesized to biological activity of natural products, chiral auxiliaries, antibiotics and drugs. For this reason, this reaction can be applied in the field of fine chemicals and biopharmaceuticals, and has an important application in industrial research. However, the activity of the aromatic amine is lower than that of the aliphatic amine in  $\alpha$ ,  $\beta$ -unsaturated carbonyl compounds addition reactions. Thus, Aza-Michael reaction of weak amphiphilic aromatic amines is reported less than that of aliphatic amines. Therefore, it is significant to be studied.

Lewis acid catalysts are often used in the Aza-Michael reaction, such as ionic liquids<sup>[4]</sup>, transition metal salts<sup>[5]</sup>, Pd( $N,N'$ -ppo)Cl<sub>2</sub><sup>[6]</sup>, samarium diiodide<sup>[7]</sup>, Zn/InCl<sub>3</sub><sup>[8]</sup>, heterocyclic carbenes<sup>[9]</sup>. These catalysts have a number of disadvantages. For example, the use of large amount of catalyst, the recycling and separation of catalysts from solution after reaction are difficult, and their disposal after use would cause environmental pollution. From this point of view, many researchers have converted their focus to heterogeneous catalysts. Mokhtar et al.<sup>[10]</sup> used Mg-Al hydrotalcites as a heterogeneous reusable catalyst for the synthesis of pyrazolo [1,5-*b*]pyrimidine derivatives. The pure product yield over 90% under the condition of microwave irradiation for 15 min.

Metal-organic frameworks (MOFs) are a kind of nano porous materials and have the larger surface area. These features give MOFs have great potential for heterogeneous catalysis<sup>[11]</sup>. Some MOFs with Lewis acid sites were used in Lewis acid-catalyzed reactions, such as HKUST-1, MIL-100 (Fe, Cr), MIL-101 (Fe, Cr), UiO-66, MIL-100 (Sc)<sup>[12]</sup>. Nguyen et al.<sup>[13]</sup> used MOF-199 as an efficient heterogeneous catalyst for the Aza-

Michael reaction of benzylamine with ethyl acrylate. Excellent conversions were achieved under mild reaction conditions in the presence of 5% (*n/n*) catalyst.

Recently, our group also focuses the Lewis acid catalytic activity of MOFs<sup>[14,18-21]</sup>, especially magnetic MOF@Fe<sub>3</sub>O<sub>4</sub> with Lewis acid which is easy to recycle. Currently, the magnetic MOF@Fe<sub>3</sub>O<sub>4</sub> is widely used for drug delivery, environmental control, catalysis, sensing and miniaturized device fabrication<sup>[15]</sup>. However, it is difficult to synthesis the MOF@Fe<sub>3</sub>O<sub>4</sub> with regular structures. To solve this problem, the Fe<sub>3</sub>O<sub>4</sub> are encapsulated into SiO<sub>2</sub>. It is facilitated the *in-situ* growth of the MOF material with regular structures for silanol moieties on the SiO<sub>2</sub> surface greatly contribute to the hydrophilic property of silica<sup>[16-17]</sup>, meanwhile helps to protect Fe<sub>3</sub>O<sub>4</sub> from oxidation<sup>[14]</sup>. Therefore, our group prepared a series of magnetic MOF@SiO<sub>2</sub>@Fe<sub>3</sub>O<sub>4</sub> such as the Cu-BTC@SiO<sub>2</sub>@Fe<sub>3</sub>O<sub>4</sub> (BTC is benzene-1,3,5-tricarboxylic acid) catalyst for the Pechmann reaction of 1-naphthol with ethyl acetoacetate<sup>[18]</sup>, the Zn-BTC@SiO<sub>2</sub>@Fe<sub>3</sub>O<sub>4</sub> catalyst for the toluene acylation with *p*-toluoyl chloride<sup>[19]</sup>, the MOF-5@SiO<sub>2</sub>@Fe<sub>3</sub>O<sub>4</sub> catalyst for the Friedel-Crafts alkylation of toluene with benzyl chloride<sup>[20]</sup>, the MIL-53(Al)@SiO<sub>2</sub>@Fe<sub>3</sub>O<sub>4</sub> catalyst for Friedel-Crafts acylation reaction of 2-methylindole with benzoyl chloride<sup>[21]</sup>, etc.

Lanthanide organic frameworks (Ln-MOFs) are an important rare earth metal MOF material. Because its crystal has special structure of topology, Ln-MOFs has great potentials in high performance light emitting devices<sup>[22-23]</sup>, magnetic materials<sup>[24]</sup>, catalyst fields<sup>[25]</sup>. Ln-MOFs also exhibit the Lewis acid sites<sup>[26]</sup> and Y-MOF has high thermal stability<sup>[27]</sup>. In this work, the magnetic Y-MOF@SiO<sub>2</sub>@Fe<sub>3</sub>O<sub>4</sub> catalysts with different Y-MOF contents were synthesized. The structure of the catalyst was characterized. The performance of the catalyst for the Aza-Michael addition reaction of aniline with methyl acrylate was evaluated.

## 1 Experimental

### 1.1 Synthesis of magnetic Y-MOF@SiO<sub>2</sub>@Fe<sub>3</sub>O<sub>4</sub> catalyst

The synthesis of magnetic SiO<sub>2</sub>@Fe<sub>3</sub>O<sub>4</sub> support

was carried out according to the literatures<sup>[21]</sup>. The SiO<sub>2</sub> was coated on the surface of magnetic Fe<sub>3</sub>O<sub>4</sub> nanoparticles for protecting Fe<sub>3</sub>O<sub>4</sub> and preventing it from oxidation<sup>[28]</sup>. The Y-MOF was synthesis according to the procedure described by Liu et al<sup>[29]</sup>. The Y-MOF@SiO<sub>2</sub>@Fe<sub>3</sub>O<sub>4</sub> catalyst was prepared as follows: An amount of SiO<sub>2</sub>@Fe<sub>3</sub>O<sub>4</sub> was dispersed in a mixture of Y(NO<sub>3</sub>)<sub>3</sub>·6H<sub>2</sub>O, Trimesic acid (H<sub>3</sub>BTC), *N,N*-dimethylformamide (DMF) and H<sub>2</sub>O by ultrasonic method. Then the solution was transferred to a Teflon-lined steel autoclave and kept at 100 °C for 12 h. After reaction, the formed powder was separated by an external magnet and washed several times with distilled water. Finally, solids were dried at 60 °C for 8 h under vacuum. Slightly gray-white solid Y-MOF@SiO<sub>2</sub>@Fe<sub>3</sub>O<sub>4</sub> magnetic catalyst was obtained. The magnetic Y-MOF@SiO<sub>2</sub>@Fe<sub>3</sub>O<sub>4</sub> catalysts with Y-MOF contents of 15.2%, 26.1%, 33.5%, 43.3% and 58.8% (*w/w*) were named as YM-1, YM-2, YM-3, YM-4 and YM-5, respectively.

## 1.2 Characterizations of Y-MOF@SiO<sub>2</sub>@Fe<sub>3</sub>O<sub>4</sub> catalyst

X-ray diffraction (XRD) patterns of samples were obtained on a Rigaku D/MAX-2500VPC with Cu K $\alpha$  radiation ( $\lambda=0.154\ 18\ \text{nm}$ ) at 200 kV and 50 mA with a graphite monochromator and scans between 5°~80°. Transmission electron microscopy (TEM) was performed on a JEOL (JEM 2100) transmission emission microscope operated at 200 kV accelerating voltage. Fourier transform infrared spectroscopy (FT-IR) was carried out on a Bruker Tensor-27 using KBr pellet samples. The magnetic property of the samples was measured using a vibration sample magnetometer (VSM, Laker shore Model 7400) under magnetic fields up to 20 kOe. The N<sub>2</sub> adsorption-desorption isotherm were measured on an on an ASAP 2020M automatic specific surface area and aperture analyzer.

## 1.3 Catalytic evaluation for Aza-Micheal addition reaction

Aza-Micheal addition reaction was carried out in an Eggplant type flask with a condenser and stirring. A certain amount of aniline, methyl acrylate, the catalysts and n-dodecane were added in the flask and

stirred at a certain temperature for specific time intervals. After reaction, the catalyst was separated from the solvent by an external magnet. The supernatant liquid was analyzed by a GC (Beijing Beifen-ruli Analytical Instrument Co., Ltd., SP-4000A with FID ionization detector). The GC instrument was equipped with a capillary column named as HJ. PONA, 50 m×0.2 mm×0.50  $\mu\text{m}$ . The injector temperature was 240 °C, and the detector temperature was 250 °C. According to the program for GC analysis, the sample was heated from 100 °C and was held at the same temperature for 1 min, then from 100 to 240 °C at a heating speed of 10 °C·min<sup>-1</sup>, and was held at 240 °C for 10 min. After reaction, the liquid was poured from the flask, the magnetic Y-MOF@SiO<sub>2</sub>@Fe<sub>3</sub>O<sub>4</sub> catalyst was separated by an external magnet and washed several times with ethanol. Finally, the catalysts were activated at 150 °C under vacuum. Then the recovered catalyst was added to the flask reactor and used for the next run. The conversion of methyl acrylate (C), the selectivity (S) and the yield (Y) of *N*-( $\beta$ -methoxycarbonyl) ethyl) aniline were all calculated with n-dodecane as an internal standard.

## 2 Results and discussion

### 2.1 Structure of Y-MOF@SiO<sub>2</sub>@Fe<sub>3</sub>O<sub>4</sub> catalysts

XRD patterns of Y-MOF@SiO<sub>2</sub>@Fe<sub>3</sub>O<sub>4</sub> catalysts with different Y-MOF contents, Fe<sub>3</sub>O<sub>4</sub>, SiO<sub>2</sub>@Fe<sub>3</sub>O<sub>4</sub> and simulated Y-MOF were shown in Fig.1. The Fe<sub>3</sub>O<sub>4</sub> shows strong characteristic diffraction peaks at 30.0°, 35.6°, 43.4°, 57.4° and 62.8° (Fig.1(a)). These peaks are ascribed to the typical cubic spinel structure of Fe<sub>3</sub>O<sub>4</sub> and consistent with PDF No.88-0866<sup>[30]</sup>. The XRD patterns of SiO<sub>2</sub>@Fe<sub>3</sub>O<sub>4</sub> shows strong diffraction peaks of Fe<sub>3</sub>O<sub>4</sub> (Fig.1(b)). The peak type and peak intensity of Fe<sub>3</sub>O<sub>4</sub> do not change significantly, but there is a weak diffusion diffraction peak, which appeared between 15° and 30°, which may be the characteristic diffraction peak of the coated SiO<sub>2</sub><sup>[31]</sup>. The XRD pattern of synthesized Y-MOF shows strong diffraction peaks at 6.6°, 10.6°, 18.3°, 19.3°, 20.3°, 25.3°, 26.8°, 27.5° and 28.16° (Fig.1(h)), and consistent with simulated Y-MOF (Fig.1(i)). It proves that the synthesized MOF

is Y-MOF<sup>[29,32]</sup>. The XRD patterns of the magnetic Y-MOF@SiO<sub>2</sub>@Fe<sub>3</sub>O<sub>4</sub> catalysts with different contents of Y-MOF show (Fig.1(c~g)) the characteristic diffraction of Y-MOF. This indicates that the Y-MOF@SiO<sub>2</sub>@Fe<sub>3</sub>O<sub>4</sub> still has a complete structure of Y-MOF<sup>[29]</sup>. With the increase of the Y-MOF content of magnetic Y-MOF@SiO<sub>2</sub>@Fe<sub>3</sub>O<sub>4</sub> catalyst, the Y-MOF characteristic diffraction peak intensity gradually increases, and the diffraction peak intensity of Fe<sub>3</sub>O<sub>4</sub> gradually decreases, and no obvious diffraction of SiO<sub>2</sub>.

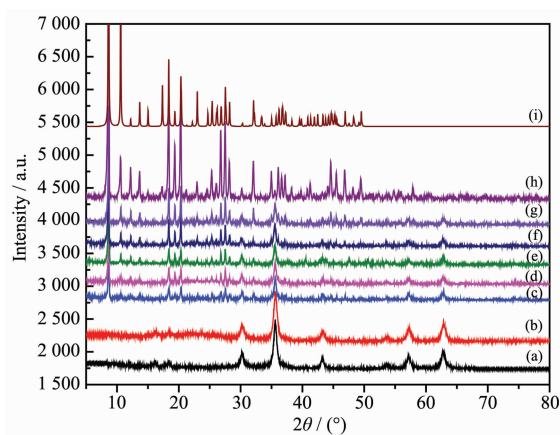


Fig.1 XRD patterns of (a) Fe<sub>3</sub>O<sub>4</sub>, (b) SiO<sub>2</sub>@Fe<sub>3</sub>O<sub>4</sub>, (c) YM-1, (d) YM-2, (e) YM-3, (f) YM-4, (g) YM-5, (h) as-synthesized Y-MOF and (i) simulated Y-MOF

The TEM of the samples are shown in Fig.2. The magnetic Y-MOF@SiO<sub>2</sub>@Fe<sub>3</sub>O<sub>4</sub> catalysts have a uniform particle size between 140 and 200 nm. It presents a

relatively regular spherical core-shell structure. As the amount of Y-MOF coating increases, the thickness of the shell gradually increases.

The FT-IR spectra of Y-MOF@SiO<sub>2</sub>@Fe<sub>3</sub>O<sub>4</sub> catalysts with different contents of Y-MOF and the ligands H<sub>3</sub>BTC are shown in Fig.3. The strong vibration peak at 1 691 and 1 280 cm<sup>-1</sup> in Fig.3(a) can be ascribed to stretching vibration of C=O bond of COOH in organic ligand H<sub>3</sub>BTC. The bands appear at 2 500~3 300 cm<sup>-1</sup> are assigned to the stretching vibrations of O-H bonds of -OH in water<sup>[33]</sup>. The sharp peak at 750~900 cm<sup>-1</sup> are attributed to the bending vibration of O-H bond<sup>[33]</sup>. Two bands at 1 276 and 1 117 cm<sup>-1</sup> are assigned to the bending vibration of C-H bond in benzene ring<sup>[34]</sup>. The FT-IR spectrum of Y-MOF@SiO<sub>2</sub>@Fe<sub>3</sub>O<sub>4</sub> has no peak near 1 690 cm<sup>-1</sup>, indicating that there is no free H<sub>3</sub>BTC molecule in the sample. The bands that appear at 1 400~1 700 cm<sup>-1</sup> are assigned to asymmetric stretching vibration (1 608 and 1 507 cm<sup>-1</sup>) and symmetric stretching vibration (1 445 and 1 417 cm<sup>-1</sup>) of -COO in organic ligands of Y-MOF<sup>[35]</sup>, and the band which appears at 570 cm<sup>-1</sup> is assigned to vibration of Y-O bond<sup>[29]</sup>.

VSM analysis of the samples are shown in Fig.4. The magnetization saturation of Fe<sub>3</sub>O<sub>4</sub> is 81.9 emu·g<sup>-1</sup>, and the magnetization saturation of SiO<sub>2</sub>@Fe<sub>3</sub>O<sub>4</sub> is 77.0 emu·g<sup>-1</sup>, lower than that of Fe<sub>3</sub>O<sub>4</sub>. This behavior

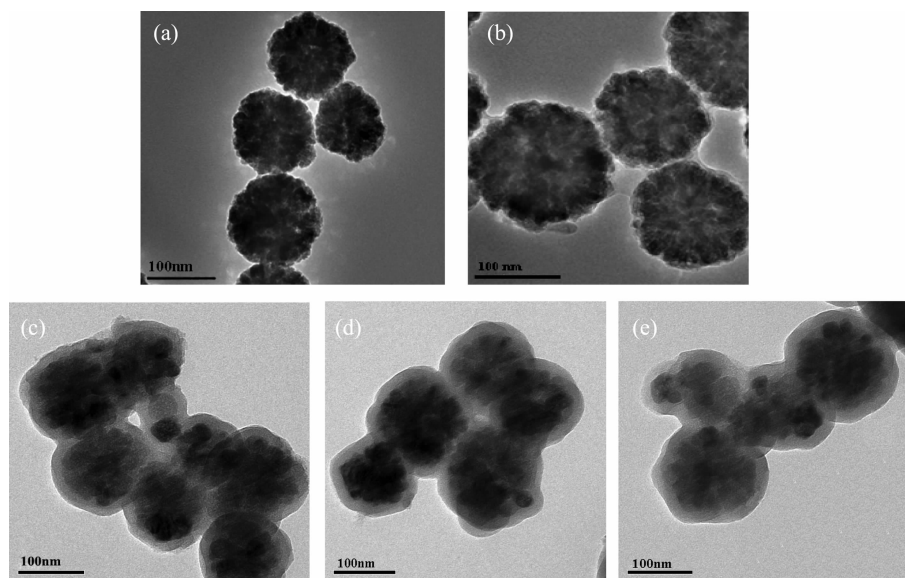


Fig.2 TEM images of (a) Fe<sub>3</sub>O<sub>4</sub>, (b) SiO<sub>2</sub>@Fe<sub>3</sub>O<sub>4</sub> (c) YM-3, (d) YM-4 and (e) YM-5



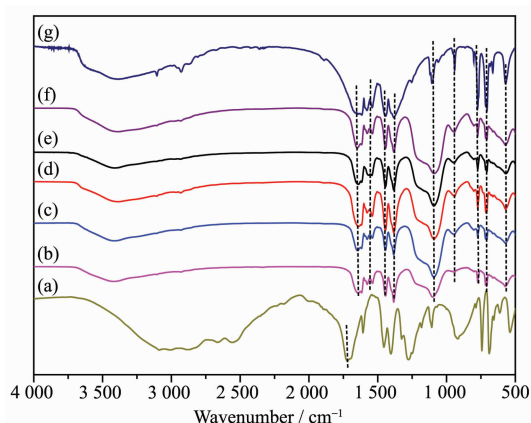


Fig.3 FT-IR spectra of (a) H<sub>3</sub>BTC, (b) YM-1, (c) YM-2, (d) YM-3, (e) YM-4, (f) YM-5 and (g) Y-MOF

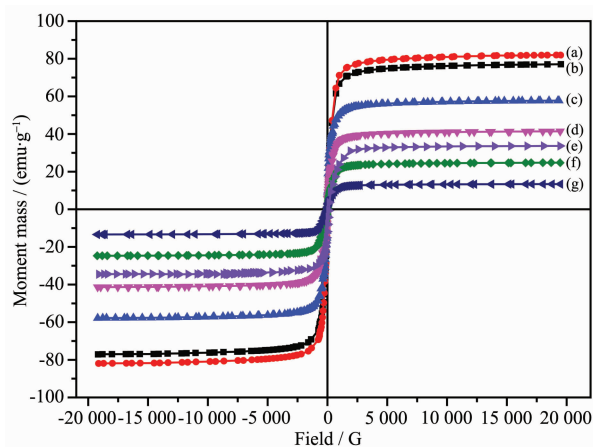


Fig.4 VSM of (a) Fe<sub>3</sub>O<sub>4</sub>, (b) SiO<sub>2</sub>@Fe<sub>3</sub>O<sub>4</sub>, (c) YM-1, (d) YM-2, (e) YM-3, (f) YM-4 and (g) YM-5

is mainly due to the encapsulated SiO<sub>2</sub> layer on the surface of Fe<sub>3</sub>O<sub>4</sub> particles. The magnetization saturation of all the magnetic Y-MOF@SiO<sub>2</sub>@Fe<sub>3</sub>O<sub>4</sub> catalysts with superparamagnetism is lower than that of SiO<sub>2</sub>@Fe<sub>3</sub>O<sub>4</sub>. The magnetization saturation decreases gradually with the increase of Y-MOF content in the catalyst. Due to the gradual increase of the thickness of the shell with the increase of the amount of Y-MOF coating, the magnetization saturation decreases gradually. This is consistent with the results of the work of Jiang et al<sup>[21]</sup>. The magnetization saturation of YM-1, YM-2, YM-3, YM-4 and YM-5 is 57.7, 41.4, 33.65, 24.7 and 13.4

emu · g<sup>-1</sup>, respectively. Although the magnetization of YM-5 is minimal, rapid separation is still possible under an external magnetic field.

The N<sub>2</sub> adsorption-desorption isotherm of the samples had been shown in Table 1. The BET surface area ( $S_{\text{BET}}$ ) of Y-MOF was 592 m<sup>2</sup> · g<sup>-1</sup>. With further encapsulation of different contents of Y-MOF, the surface areas of the as-synthesized catalysts were decreased. The BET surface area of Y-MOF@SiO<sub>2</sub>@Fe<sub>3</sub>O<sub>4</sub> with different contents of Y-MOF was from 141 to 389 m<sup>2</sup> · g<sup>-1</sup>. It can be seen that the pore size distribution ( $D$ ) was mainly between 1.1 and 1.2 nm.

Table 1 BET surface area ( $S_{\text{BET}}$ ) and pores data ( $D$ ) of the samples

Sample	Content of Y-MOF / %	$S_{\text{BET}}$ / (m <sup>2</sup> · g <sup>-1</sup> )	$D$ / nm
YM-1	15.2	141	1.2
YM-2	26.1	194	1.2
YM-3	33.5	230	1.1
YM-4	43.3	298	1.2
YM-5	58.8	389	1.2
Y-MOF	100	592	1.3

## 2.2 Performance of the catalysts for Aza-Michael addition reaction

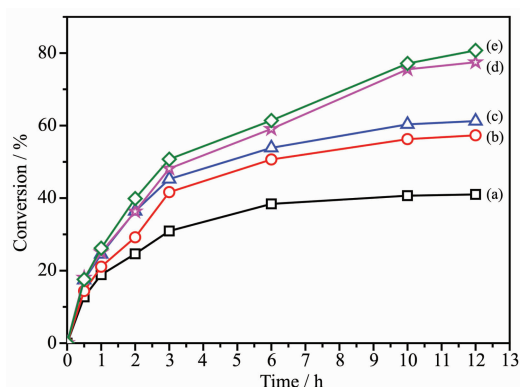
Scheme 1 is Aza-Michael reaction equation using the aniline and methyl acrylate as reactants over the Y-MOF@SiO<sub>2</sub>@Fe<sub>3</sub>O<sub>4</sub> catalyst.

After some test of the catalytic performance for Aza-Michael addition reaction were conducted. In this part, the effect of catalysts and reaction time, the reaction temperature, the values of  $n_{\text{catalyst}}/n_{\text{methyl acrylate}}$  and  $n_{\text{aniline}}/n_{\text{methyl acrylate}}$ , and the recovery and reuse times on catalytic performance over YM-4 catalyst were investigated. The results of the catalytic performance over Y-MOF@SiO<sub>2</sub>@Fe<sub>3</sub>O<sub>4</sub> with different Y-MOF contents are shown in Fig.5. It can be seen that the conversion of methyl acrylate increased with the increase in reaction time. Within 3.0 h, the conversion rate increased rapidly. When the reaction time was more than 3.0 h,



Scheme 1 Aza-Michael addition reaction equation of aromatic amines to  $\alpha$ ,  $\beta$ -unsaturated compounds

the conversion rate increased slowly and the conversion reached the highest value at 12 h. In the absence of the addition of the catalyst, it was observed that the reaction did not occur and the conversion was 0. Using Y-MOF@SiO<sub>2</sub>@Fe<sub>3</sub>O<sub>4</sub> as catalyst, the conversion of Aza-Micheal reaction increased with the increase of Y-MOF content. When YM-5 was used as catalyst, the conversion of methyl acrylate was the highest and the conversion was 80.7% at 12 h. However, the conversion of YM-4 was 77.5% lower than that of YM-5, but the difference was very small.



Reaction conditions:  $n_{\text{aniline}}/n_{\text{methyl acrylate}}=2.0$ ,  $n_{\text{catalyst}}/n_{\text{methyl acrylate}}=0.14$ , 80 °C

Fig.5 Catalytic performance of (a) YM-1, (b) YM-2, (c) YM-3, (d) YM-4 and (e) YM-5 at different times

Therefore, in this paper, the YM-4 catalyst was chosen and used for catalyst activity evaluation. However, the time over 10 h, the rate of conversion increased become slowly. So, the best reaction time was 10 h.

The results of the catalytic performance over the YM-4 catalyst on different  $n_{\text{catalyst}}/n_{\text{methyl acrylate}}$  are shown in Table 2. When the  $n_{\text{catalyst}}/n_{\text{methyl acrylate}}$  was below 0.18, the conversion of methyl acrylate and the yield of product increased with the increase of  $n_{\text{catalyst}}/n_{\text{methyl acrylate}}$ . When the  $n_{\text{catalyst}}/n_{\text{methyl acrylate}}$  was 0.18, the conversion of methyl acrylate was 86.1%, and the yield of product was 86.0%. When the  $n_{\text{catalyst}}/n_{\text{methyl acrylate}}$  was increased to 0.22, the conversion and yield were the highest and reached 88.2% and 88.0%, respectively. Thus, the  $n_{\text{catalyst}}/n_{\text{methyl acrylate}}=0.18$  can meet the current reaction requirement. When the  $n_{\text{catalyst}}/n_{\text{methyl acrylate}}$  further increased, the conversion and yield were not significantly improved. Thus, the optimum the  $n_{\text{catalyst}}/n_{\text{methyl acrylate}}$  was 0.18.

The results of the catalytic performance over the YM-4 catalyst at different reaction temperatures are shown in Table 3. The reaction temperature had a great effect on the Aza-Micheal addition reaction of aniline and methyl acrylate. When the reaction temperature was 50 °C, the conversion of methyl acrylate

Table 2 Effect of  $n_{\text{catalyst}}/n_{\text{methyl acrylate}}$  on catalytic performance

$n_{\text{catalyst}}/n_{\text{methyl acrylate}}$	$C / \%$	$S / \%$	$Y / \%$	TOF / h <sup>-1</sup>
0.02	54.9	99.8	54.8	6.60
0.06	54.1	99.2	53.7	5.10
0.10	66.2	99.9	66.1	4.01
0.14	75.5	99.5	75.2	3.27
0.18	86.1	99.8	86.0	2.77
0.22	88.2	99.8	88.0	2.01

Reaction conditions:  $n_{\text{aniline}}/n_{\text{methyl acrylate}}=2.0$ , 80 °C, 10 h

Table 3 Catalytic performance at different reaction temperatures

$T / ^\circ\text{C}$	$C / \%$	$S / \%$	$Y / \%$
50	53.6	98.9	53.0
60	58.5	99.7	58.4
70	79.6	99.5	79.2
80	86.1	99.8	86.0
90	73.1	99.6	72.9
100	65.4	99.8	65.3

Reaction conditions:  $n_{\text{aniline}}/n_{\text{methyl acrylate}}=2.0$ ,  $n_{\text{catalyst}}/n_{\text{methyl acrylate}}=0.18$ , 10 h.

and the yield of the product were low, because the reaction proceeded very slowly at lower temperatures. The conversion of methyl acrylate and the yield of the product increased with increasing temperature. When the reaction temperature was 80 °C, the conversion and yield were the highest and have reached 86.1% and 86.0%, respectively. After the reaction temperature was beyond 80 °C, the conversion of methyl acrylate and the yield of the product began to decline significantly. It is speculated that the reason may be that an excessively high temperature is not conducive to the stabilization of the skeletal structure of the Y-MOFs in the magnetic composite catalyst. Therefore, the most suitable reaction temperature was 80 °C.

The results of the catalytic performance on the molar ratios of aniline to methyl acrylate over the YM-4 catalyst are shown in Table 4. When  $n_{\text{aniline}}/n_{\text{methyl acrylate}}$  was 1.0, the conversion of methyl acrylate and the yield of the product were lower, and merely achieved

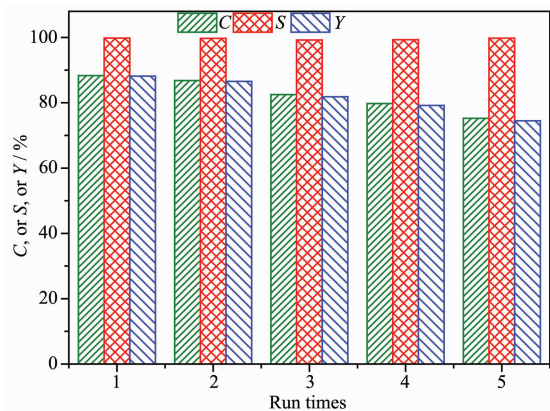
63.2% and 63.0%, respectively. When  $n_{\text{aniline}}/n_{\text{methyl acrylate}}$  was below 2.5, the conversion of methyl acrylate and the yield of the product was proportional to the molar ratio of aniline to methyl acrylate. When  $n_{\text{aniline}}/n_{\text{methyl acrylate}}$  was 2.5, the conversion of methyl acrylate and the yield of the product were high, and reached 88.3% and 88.1%, respectively. When the amount of aniline was increased, the conversion of methyl acrylate and the yield of the product decreased with the increase of aniline to methyl acrylate molar ratio. This may be due to the excessive amount of aniline reduced the concentration of methyl acrylate during the reaction. Aniline can be used as a solvent. The selectivity of the product was less affected by the molar ratios of aniline to methyl acrylate and was maintained in the range of 98.9% to 99.8%. Thus, the optimum molar ratio between aniline and methyl acrylate is  $n_{\text{aniline}}/n_{\text{methyl acrylate}}$  was 2.5.

**Table 4** Effect of molar ratio between aniline and methyl acrylate on catalytic performance

$n_{\text{aniline}}/n_{\text{methyl acrylate}}$	$C / \%$	$S / \%$	$Y / \%$
1.0	63.2	99.8	63.0
1.5	74.8	98.9	74.0
2.0	86.1	99.8	86.0
2.5	88.3	99.8	88.1
3.0	61.8	99.6	61.6

Reaction conditions:  $n_{\text{catalyst}}/n_{\text{methyl acrylate}}=0.18$ , 80 °C, 10 h.

The reusability of Y-MOF@SiO<sub>2</sub>@Fe<sub>3</sub>O<sub>4</sub> catalyst are shown in Fig.6. After reuse five times, the conversion of methyl acrylate reaction was reduced from



Reaction conditions:  $n_{\text{aniline}}/n_{\text{methyl acrylate}}=2.5$ ,  $n_{\text{catalyst}}/n_{\text{methyl acrylate}}=0.18$ , 80 °C, 10 h

**Fig.6** Reusability of the Y-MOF@SiO<sub>2</sub>@Fe<sub>3</sub>O<sub>4</sub> catalysts

88.3% to 75.2%, and the yield of product was reduced from 88.1% to 74.5%, while the selectivity of product remained at 99.8%~99.2%. It was indicated that the catalyst has a good reusability performance. We speculate that the decline of catalytic performance is mainly due to the loss of the catalyst and the long-term high-temperature drying leading to the destruction of its skeleton structure.

### 3 Conclusions

The Y-MOF was uniformly coated on the surface of magnetic SiO<sub>2</sub>@Fe<sub>3</sub>O<sub>4</sub> nanospheres through *in-situ* method to form a core-shell magnetic Y-MOF@SiO<sub>2</sub>@Fe<sub>3</sub>O<sub>4</sub> catalyst with a controlled particle size ranging from 140 to 200 nm. The magnetization saturation of the magnetic Y-MOF@SiO<sub>2</sub>@Fe<sub>3</sub>O<sub>4</sub> catalysts with

different Y-MOF contents was between 13.4~57.7 emu  $\cdot$ g<sup>-1</sup>. After reaction the magnetic catalyst can be quickly separated by the external magnetic field. In Aza-Michael addition reaction of aniline and methyl acrylate, the Y-MOF@SiO<sub>2</sub>@Fe<sub>3</sub>O<sub>4</sub> catalysts exhibited a good catalytic performance. Under the reaction conditions: the  $n_{\text{aniline}}/n_{\text{methyl acrylate}}$  was 0.18,  $n_{\text{aniline}}/n_{\text{methyl acrylate}}$  was 2.5, reaction temperature was 80 °C, reaction time was 10 h, the conversion of methyl acrylate was 88.3% and the selectivity of *N*-( $\beta$ -methoxycarbonylethyl) aniline was 99.8% over the 43.3% (*w/w*) Y-MOF@SiO<sub>2</sub>@Fe<sub>3</sub>O<sub>4</sub> catalyst. After reaction, the catalyst can be separated by the external magnetic field and reused five times still has high conversion and selectivity.

**Acknowledgments:** This work was supported by the National Natural Science Foundation of China (Grant No. 21573015, 21173018).

## References:

- [1] Ying A, Li Z F, Yang J G, et al. *J. Org. Chem.*, **2014**,**79**(14): 6510-6516
- [2] Robiette R, Tran T V, Cordi A, et al. *Synthesis*, **2010**,**2010** (18):3138-3142
- [3] Bassam N, Laure C, Jean-Francois B, et al. *Green Chem.*, **2013**,**15**(7):1900-1909
- [4] Szánti-Pintér E, Maksó L, Gömöry Á, et al. *Steroids*, **2017**, **123**:61-66
- [5] Zhang J L, Zhang Y L, Liu X H, et al. *Adv. Synth. Catal.*, **2014**,**356**(17):3545-3551
- [6] Ardizzoia G A, Brenna S, Therrien B. *Dalton Trans.*, **2012**, **41**(3):783-790
- [7] Didier D, Meddour A, Bezzenine-Lafollée S, et al. *Eur. J. Org. Chem.*, **2011**(14):2678-2684
- [8] Siddiqui I R, Shamim S, Kumar D, et al. *New J. Chem.*, **2012**,**36**:2209-2214
- [9] Kang Q, Zhang Y G. *Org. Biomol. Chem.*, **2011**,**9**(19):6715-6720
- [10] Mokhtar M, Saleh T S, Basahel S N. *J. Mol. Catal. A: Chem.*, **2012**,**353**:122-131
- [11] Jie L, Liang Z B, Zou R Q, et al. *Adv. Mater.*, **2017**,**29**(30): 17011-17032
- [12] Mitchell L, Williamson P, Ehrlichová B, et al. *Chem. Eur. J.*, **2014**,**20**:17185-17197
- [13] Nguyen L T L, Nguyen T T, Nguyen K D, et al. *Appl. Catal., A*, **2012**,**425-426**:44-52
- [14] WANG Yue(王锐), GONG Yong(龚勇), XU Hai-Juan(许海娟), et al. *Chinese J. Inorg. Chem.*(无机化学学报), **2018**,**34** (5):906-916
- [15] Ricco R, Malfatti L, Takahashi M, et al. *J. Mater. Chem. A*, **2013**,**1**(42):13033-13045
- [16] Zhu Q L, Xu Q. *Chem. Soc. Rev.*, **2014**,**43**(16):5468-5512
- [17] Huang L, Cai J, He M, et al. *Ind. Eng. Chem. Res.*, **2018**, **57**(18):6201-6209
- [18] Li Q Y, Jiang S, Ji S F, et al. *Ind. Eng. Chem. Res.*, **2014**, **53**(39):14948-14955
- [19] LI Qing-Yuan(李庆远), MUHAMMAD Ammar, JI Sheng-Fu(季生福), et al. *Acta Petrolei Sinica*(石油学报(石油加工)), **2014**,**30**(1):126-133
- [20] Li Q Y, Jiang S, Ji S F, et al. *J. Porous Mater.*, **2015**,**22**(5): 1205-1214
- [21] Jiang S, Yan J L, Habimana F, et al. *Catal. Today*, **2016**, **264**:83-90
- [22] Shen L L, Yang L, Fan Y, et al. *CrystEngComm*, **2015**,**17** (48):9363-9369
- [23] Wang S Y, Shan L, Fan Y, et al. *J. Solid State Chem.*, **2017**, **245**:132-137
- [24] Datcu A, Roques N, Jubera V, et al. *Chem. Eur. J.*, **2011**,**17** (13):3644-3656
- [25] Chen Y, Ma S. *Rev. Inorg. Chem.*, **2012**,**32**:81-100
- [26] Pagis C, Ferbinteanu M, Rothenberg G. *ACS Catal.*, **2016**,**6**: 6063-6072
- [27] Luo J H, Xu H W, Liu Y, et al. *J. Am. Chem. Soc.*, **2008**, **130**:9626-9627
- [28] YANG Qing-Xiang(杨清香), REN Shuang-Shuang(任爽爽), ZHAO Qian-Qian(赵倩倩), et al. *Chinese J. Inorg. Chem.* (无机化学学报), **2017**,**33**(5):843-852
- [29] Liu X, Wang J Y, Li Q Y, et al. *J. Rare. Earths.*, **2014**,**32** (2):189-194
- [30] Liu H F, Zeng P H, Ji S F, et al. *Catal. Today*, **2011**,**175**(1): 293-298
- [31] Ji J H, Zeng P H, Ji S F, et al. *Catal. Today*, **2010**,**158**(3): 305-309
- [32] Zou X Q, Goupil J M, Thomas S, et al. *J. Phys. Chem. C*, **2012**,**116**(31):16593-16600
- [33] Shu Y, Meng Y, Chen M L, et al. *Chin. Chem. Lett.*, **2015**, **26**(12):1460-1464
- [34] Mahalakshmi G, Balachandran V. *Spectrochim. Acta, Part A*, **2014**,**124**(8):535-547
- [35] Wang F, Deng K J, Wu G L, et al. *J. Inorg. Organomet. Polym.*, **2012**,**22**(4):680-685